Journal of Experimental Botany, Vol. 62, No. 13, pp. 4481–4493, 2011
doi:10.1093/jxb/err145 Advance Access publication 30 May, 2011
This paper is available online free of all access charges (see http://jxb.oxfordjournals.org/open_access.html for further details)

Journal of Experimental Botany
www.jxb.oxfordjournals.org

RESEARCH PAPER

Hydrogen sulphide enhances photosynthesis through promoting chloroplast biogenesis, photosynthetic enzyme expression, and thiol redox modification in *Spinacia oleracea* seedlings

Juan Chen[1,*], Fei-Hua Wu[1,2,*], Wen-Hua Wang[1], Chen-Juan Zheng[1], Guang-Hui Lin[1], Xue-Jun Dong[3], Jun-Xian He[4], Zhen-Ming Pei[2,1] and Hai-Lei Zheng[1,†]

[1] Key Laboratory for Subtropical Wetland Ecosystem Research of MOE, School of Life Sciences, Xiamen University, Xiamen, Fujian 361005, PR China
[2] Department of Biology, Duke University, Durham, NC 27708, USA
[3] Central Grasslands Research Extension Center, North Dakota State University, Streeter, ND 58483, USA
[4] State Key Laboratory of Agobiotechnology and School of Life Sciences, The Chinese University of Hong Kong, Hong Kong, PR China

* These authors contributed equally to this work.
† To whom correspondence should be addressed. E-mail: zhenghl@xmu.edu.cn

Received 24 January 2011; Revised 27 March 2011; Accepted 11 April 2011

Abstract

Hydrogen sulphide (H_2S) is emerging as a potential messenger molecule involved in modulation of physiological processes in animals and plants. In this report, the role of H_2S in modulating photosynthesis of *Spinacia oleracea* seedlings was investigated. The main results are as follows. (i) NaHS, a donor of H_2S, was found to increase the chlorophyll content in leaves. (ii) Seedlings treated with different concentrations of NaHS for 30 d exhibited a significant increase in seedling growth, soluble protein content, and photosynthesis in a dose-dependent manner, with 100 μM NaHS being the optimal concentration. (iii) The number of grana lamellae stacking into the functional chloroplasts was also markedly increased by treatment with the optimal NaHS concentration. (iv) The light saturation point (*L*sp), maximum net photosynthetic rate (*P*max), carboxylation efficiency (*CE*), and maximal photochemical efficiency of photosystem II (F_v/F_m) reached their maximal values, whereas the light compensation point (*L*cp) and dark respiration (*R*d) decreased significantly under the optimal NaHS concentration. (v) The activity of ribulose-1,5-bisphosphate carboxylase (RuBISCO) and the protein expression of the RuBISCO large subunit (RuBISCO LSU) were also significantly enhanced by NaHS. (vi) The total thiol content, glutathione and cysteine levels, internal concentration of H_2S, and *O*-acetylserine(thiol)lyase and L-cysteine desulphydrase activities were increased to some extent, suggesting that NaHS also induced the activity of thiol redox modification. (vii) Further studies using quantitative real-time PCR showed that the gene encoding the RuBISCO large subunit (*RBCL*), small subunit (*RBCS*), ferredoxin thioredoxin reductase (*FTR*), ferredoxin (*FRX*), thioredoxin m (*TRX-m*), thioredoxin f (*TRX-f*), NADP-malate dehydrogenase (*NADP-MDH*), and *O*-acetylserine(thiol)lyase (*OAS*) were up-regulated, but genes encoding serine acetyltransferase (*SERAT*), glycolate oxidase (*GYX*), and cytochrome oxidase (*CCO*) were down-regulated after exposure to the optimal concentration of H_2S. These findings suggest that increases in RuBISCO activity and the function of thiol redox modification may underlie the amelioration of photosynthesis and that H_2S

Abbreviations: *AQE*, quantum yields; *CE*, carboxylation efficiency; *CCO*, cytochrome oxidase; Ci, intercellular CO_2 concentration; F_m, maximal fluorescence yield. F_o, minimal fluorescence yield; *FRX*, ferredoxin; *FTR*, ferredoxin thioredoxin reductase; *GADPH*, glyceraldehyde-3-phosphate dehydrogenase; *GYX*, glycolate oxidase; g_s, stomatal conductance; H_2S, hydrogen sulphide; LCD, L-cysteine desulphydrase; *L*cp, light compensation point; *L*sp, light saturation point; *NADP-MDH*, NADP-malate dehydrogenase; *OAS*, *O*-acetylserine(thiol)lyase gene; OAS-TL, *O*-acetylserine(thiol)lyase; PAR, photosynthetically active radiation; *P*max, maximum net photosynthetic rate; *P*n, net photosynthetic rate; PSII, photosystem II; qRT-PCR, quantitative real-time RT-PCR; *R*d, dark respiration rate; RuBISCO, ribulose-1, 5-bisphosphate carboxylase; *RBCL*, RuBISCO large subunit; *RBCS*, RuBISCO small subunit; *SERAT*, serine acetyltransferase; *TRX-f*, thioredoxin f; *TRX-m*, thioredoxin m.

plays an important role in plant photosynthesis regulation by modulating the expression of genes involved in photosynthesis and thiol redox modification.

Key words: Chloroplast ultrastructure, chlorophyll, cytochrome oxidase, glycolate oxidase, hydrogen sulphide (H_2S), photosynthesis, ribulose-1,5-bisphoshate carboxylase, *Spinacia oleracea*, thiol redox modification.

Introduction

Hydrogen sulphide (H_2S) is a colourless gas with a strong odour of rotten eggs. The toxicity of H_2S at high concentration has been substantiated for almost 300 years (Lloyd, 2006). More recently, many studies have revealed that H_2S can act as a signalling molecule similar to nitric oxide (NO) and carbon monoxide (CO) in animals at lower concentrations, and participate in various biological processes, such as smooth muscle relaxation, hippocampal long-term potentiation, brain development, blood pressure, and inflammation (Hosoki *et al.*, 1997; Wang, 2002; Li *et al.*, 2006; Yang *et al.*, 2008; Zhao *et al.*, 2001). However, there have been few studies on the involvement of H_2S in modulation of physiological processes in plant.

H_2S is thought to be released from cysteine via a reversible *O*-acetylserine(thiol)lyase (OAS-TL) reaction in plants (Sekiya *et al.*, 1982; Wirtz *et al.*, 2004). It was reported that higher plants could emit H_2S when exposed to excess sulphur and cysteine (Sekiya *et al.*, 1982; Rennenberg, 1983). Moreover, the emission of H_2S in plants is dependent on light (Wilson *et al.*, 1978). In addition, short-term exposure of *Brassica oleracea* to a high level of H_2S resulted in a decrease in the activity of adenosine 5'-phosphosulphate reductase in the shoot, and an increase in the thiol content and cysteine content in the shoot and root (Westerman *et al.*, 2000). Very recently it was reported that H_2S promotes wheat seed germination, alleviates oxidative damage against copper stress (Zhang *et al.*, 2008*a*), counteracts chlorophyll loss, and alleviates oxidative damage due to osmotic stress in sweet potato seedling leaves (Zhang *et al.*, 2009). Furthermore, boron toxicity and aluminium toxicity were alleviated by H_2S (Wang *et al.*, 2010; Zhang *et al.*, 2010). Additionally, a low H_2S concentration can promote the embryonic root length of *Pisum sativum* (Li *et al.*, 2010). All these investigations indicate that the study of H_2S in plants is just beginning.

It is well known that the increase in photosynthesis can be achieved by enhancing the activity of ribulose-1, 5-bisphosphate carboxylase (RuBISCO) (Krantev *et al.*, 2008). RuBISCO plays a cardinal role in controlling photosynthesis and is composed of eight large subunits encoded by a single gene (*RBCL*) in the chloroplast genome and eight small subunits encoded by a nuclear multigene family (*RBCS*) (Dean *et al.*, 1989). Changes in RuBISCO synthesis have been primarily explained by changes in transcript abundance of *RBCL* and *RBCS* in response to various external and/or internal signals (Nishimura *et al.*, 2008; Suzuki *et al.*, 2010). In addition, the oxidation of glycolate to glyoxylate in higher plants is catalysed by glycolate oxidase, which is located in the peroxisomes and performs an essential role in the oxidative photorespiration cycle accompanying photosynthetic CO_2 assimilation (Zelitch and Ochoa, 1953; Zelitch *et al.*, 2009). Meanwhile, photorespiration also involves a cooperative interaction among enzymes localized in chloroplasts, mitochondria, and peroxisomes, and is performed by the glycolate pathway. Glycolate oxidase is the first enzyme in this pathway (Yamaguchi and Nishimura, 2000).

A previous study has shown that NO could increase the photosynthetic rate of *Spinacia oleracea* and lead to more biomass accumulation (Jin *et al.*, 2009). Photosynthesis was altered by NO through changing the ultrastructure of chloroplasts in flax leaf blades (Batasheva *et al.*, 2010). Likewise, CO is able to prevent the iron deficiency-induced chlorosis and improve the chlorophyll accumulation in *Arabidopsis thaliana* (Kong *et al.*, 2010). As for the effect of H_2S on photosynthesis, it was reported that excess sulphide (1 mM) resulted in inhibition of photosystem II (PSII) in cyanobacteria and tobacco chloroplasts (Oren *et al.*, 1979), and that a high sulphide concentration (2 mM) depressed the growth and photosynthesis in a mangrove plant (Lin and Sternberg, 1992). However, it is not clear whether a low concentration of H_2S is involved in regulation of photosynthesis in plants.

In this study, NaHS, a donor of H_2S frequently used in animal research, was adopted to understand further the roles of H_2S in physiological processes of photosynthesis and grana lamella formation in *S. oleracea*. The results indicated that the net photosynthesis (*P*n), RuBISCO, OAS-TL, and L-cysteine desulphydrase (LCD) activities and other photosynthetic characteristics were altered by exogenous application of a low concentration of NaHS. The number of grana lamellae stacking into functional chloroplasts was also increased markedly. Furthermore, it was demonstrated that seedlings treated with 100 μM NaHS increased the expression of the genes *RBCL* and *RBCS*, and those of the ferredoxin/thioredoxin system, and the protein expression level of the RuBISCO large subunit (RuBISCO LSU), but significantly decreased the gene expression of glycolate oxidase (*GYX*) and cytochrome oxidase (*CCO*). It is concluded that H_2S acts as a signalling molecule that participates in enhancing photosynthesis and chloroplast development during *S. oleracea* growth.

Materials and methods

Plant growth and treatments

Seeds of *S. oleracea* were first sterilized in 75% ethanol for 3 min and then in 10% sodium hypochlorite solution for an additional

10 min followed by washing with distilled water and germinating in a soil/vermiculite (1:1) mixture. Two-week-old seedlings were transferred to 1/2 strength Hoagland's solution (pH 6.0) in a controlled growth chamber with a light/dark regime of 15/9 h, relative humidity of 80%, temperature of 21/27 °C, and a photosynthetically active radiation (PAR) of 190 μmol m^{-2} s^{-1}. NaHS was purchased from Sigma and used as the exogenous H_2S donor as described by Hosoki *et al.* (1997). Seedlings were divided into two groups for further treatment. In the first group, seedlings were supplied with various concentrations of NaHS (0, 10, 100, 500, and 1000 μM) for 30 d. The solutions were changed every 3 d. In the second group, seedlings were treated with the optimal concentration of NaHS (identified from the trial experiment of the first group) for 0, 6, 12, 24, and 36 h. In order to distinguish the possible roles of H_2S, HS^-, Na^+, or other sulphur-containing components in photosynthesis, a series of chemicals such as Na_2S, Na_2SO_4, Na_2SO_3, $NaHSO_4$, $NaHSO_3$, and NaAC were used as the controls of NaHS. The leaves of *S. oleracea* were collected and immediately frozen in liquid N_2 and stored at –80 °C for further analyses, with the exception that fresh leaves were used for gas exchange, transmission electron microscopy, and chlorophyll fluorescence experiments.

Electrochemical detection of H_2S

Electrochemical detection of H_2S was performed according to Benavides *et al.* (2007) using an H_2S-selective electrode (NS-ISO-H_2S PF100H, World Precision Instruments, Inc., Sarasota, FL, USA) which was connected to an APOLLO 4000 free radical analyser (World Precision Instruments, Inc.). The analogue signal from the H_2S sensor was digitized using a DUO18 four-channel data acquisition system (World Precision Instruments, Inc.) connected to a computer. A water-jacket chamber with a circulating bath and a magnetic stirrer were also used to ensure constant temperature. The H_2S electrode was inserted into the water-jacketed chamber containing a 4 ml capacity glass vial. The vial inside the chamber was sealed with a silicon cap which was punctured in the middle to allow the passage of the electrode. The sample was mixed at a constant rate and the temperature inside the chamber was maintained at 21±1 °C with the circulating bath and the water jacket. Before use, the H_2S electrode was carefully calibrated using the method recommended by the manufacturer. Then 100 μM NaHS, Na_2S, Na_2SO_4, Na_2SO_3, $NaHSO_4$, $NaHSO_3$, and NaAC were used to investigate whether there is H_2S generation by these chemicals.

Determination of chlorophyll and soluble protein contents

Chlorophyll content was measured according to Lichtenthaler (1987) with some modifications. After extraction using 10 ml of 80% (v/v) aqueous acetone, the content of total chlorophyll and the chlorophyll *a*/*b* ratio (chl *a*/*b*) were calculated from the absorbance of leaf chlorophyll extracts at 470, 646, and 663 nm. Soluble protein content was measured according to Bradford (1976) using the Bio-Rad protein assay reagent (Bio-Rad, Hercules, CA, USA) with bovine serum albumin (BSA) as the standard protein.

Determination of the content of non-protein thiols

The total content of non-protein thiols (NPTs) in plants was measured according to Del Longo *et al.* (1993) with minor modifications. A plant sample (0.2 g) was homogenized in 1 ml of 5% (w/v) sulphosalicylic acid and incubated on ice for 30 min. The homogenate was centrifuged at 8000 *g* for 15 min at 4 °C and the NPTs content in the supernatant was measured. The reaction mixture containing 200 μl of the supernatant, 2.0 ml of 0.2 M TRIS-HCl (pH 8.2), and 0.15 ml of 10 mM 5,5'-dithio-bis-(2-nitrobenzoic acid) (DTNB) was incubated at room temperature for 20 min. After incubation, the absorbance was measured at 412 nm. An aliquot without DTNB was used to adjust the spectrophotometer to zero absorbance, and glutathione (GSH) was used as standard.

Determination of glutathione and cysteine levels

Both GSH and cysteine levels in leaf tissues were determined after labelling with monobromobimane (mBBr) and separation by reverse-phase HPLC using the following procedure (Kosower *et al.*, 1987). Fresh leaves (0.1 g) were added to 1 ml of 0.1 M HCl with 0.1 g of polyvinylpolypyrrolidone (PVPP; pre-washed with 0.1 M HCl). The samples were shaken for 60 min at room temperature. After centrifugation (15 min at 20 000 *g*, 4 °C), 100 μl of the supernatant were added to 100 μl of 200 mM 2-(cyclohexylamino)ethanesulphonic acid (CHES), pH 8.5. Reduction of the total disulphides was performed by adding 70 μl of 100 mM dithiothreitol (DTT). After 1 h incubation at room temperature, free thiols were labelled with mBBr. Then 10 μl of 16 mM mBBr in acetonitrile were added to the mixture for 15 min in the dark at room temperature. The reaction was stopped by adding 220 μl of 10 mM methylsulphonic acid. The samples were centrifuged at 20 000 *g* for 40 min at 4 °C and then filtered through a 0.2 μm nylon filter, and separation of thiols was carried out on an Agilent Hypersil BDS-C18 column using an HP1100 HPLC system. Mixed standards treated exactly as the sample supernatants were used as a reference for the quantification of cysteine and GSH content.

Transmission electron microscopy

Leaves were cut into 0.5 mm×1 mm pieces and immediately fixed with 2.5% glutaraldehyde (in 0.1 M sodium phosphate buffer, pH 7.0) at room temperature for 4 h. After three 20 min rinses, the samples were post-fixed with 1% OsO_4 in the same buffer for 4 h at room temperature, followed by three buffer rinses. Samples were dehydrated in an acetone series, embedded in Spurr's resin, and sectioned with a Leica EM UC6 ultramicrotome (Leica Microsystems GmbH, Wetzlar, Germany). The ultrathin sections (70–90 nm) were stained with uranyl acetate and lead citrate. A Philips CM 100 transmission electron microscope (Philips, Eindhoven, The Netherlands) at 80 kV was used for ultrastructure imaging of chloroplasts. At least three seedlings and >30 individual chloroplasts were observed for each indicated time point by following the methods of Chang *et al.* (2008).

Gas exchange and chlorophyll fluorescence quenching analyses

The net photosynthetic rate (*P*n) and stomatal conductance (g_s) were measured using a portable photosynthesis system (Li-6400, Li-Cor, Lincoln, NE, USA) on the third fully developed leaf of each seedling. Air temperature, light intensity, CO_2 concentration, and air relative humidity were maintained at 25 °C, 800 μmol m^{-2} s^{-1} PAR, 380 μl l^{-1}, and 90%, respectively. *P*n and g_s were expressed on a leaf area basis.

Light–response curves and intercellular CO_2–response curves were also measured using the above portable photosynthesis system. Plants treated with 0 and 100 μM NaHS were measured. All measurements were conducted in the morning (9:00–11:30 h) to avoid high temperatures and the air vapour pressure deficit in the afternoon. Light was supplemented using an LED light system. The measurement was carried out on at least five leaves for both treatments in 380 μl l^{-1} CO_2 at room temperature (25 °C). The apparent dark respiration (*R*d), the light compensation point (*L*cp), the light saturation point (*L*sp), the apparent quantum yield (*AQE*), and the maximal net photosynthetic rate (*P*max) were calculated by modelling the response of leaf *P*n to PAR by a non-rectangular hyperbola, as described by Prioul and Chartier (1977).

$$Pn=\frac{AQE\times PAR+P\max-\sqrt{(AQE\times PAR+P\max)^2-4AQE\times\theta\times PAR\times P\max}}{2\theta}-Rd$$

where θ is the convexity.

The *P*n was modelled as a function of intercellular CO_2 concentration (Ci). This application fits a model curve described by the rectangular hyperbola (Olsson and Leverenz, 1994):

$$Pn=\frac{CE\times \mathrm{Ci}\times P\max}{CE\times \mathrm{Ci}+P\max}-\mathrm{Re}$$

where *P*n is the assimilation rate, *CE* is the carboxylation efficiency, Ci is the intercellular CO_2 concentration, *P*max is the assimilation at saturating CO_2, and Re is the respiratory processes (dark and light). Experimental data are fitted by first obtaining initial estimates of *CE* and Re values using linear regression over the lower part of the curve and estimating *P*max from the largest value. Subsequently a least-squares fit was obtained and values for *CE*, Re, and *P*max were presented.

Chlorophyll fluorescence was measured using a fluorescence monitoring system PAM-2100 (Heinz Walz, Effeltrich, Germany). Leaves were kept in darkness for adaptation for >30 min prior to the measurement. Two measurements were taken from each seedling to determine F_o, the initial fluorescence as all reaction centres are open, and F_m, the maximum fluorescence as all reaction centres are closed. Finally, the maximal photochemical efficiency of PSII (F_v/F_m) was calculated according to Krause and Weis (1991) using the following equation:

$$\frac{Fv}{Fm}=\frac{Fm-Fo}{Fm}$$

Measurement of endogenous H_2S

Endogenous H_2S was determined by the formation of methylene blue from dimethyl-*p*-phenylenediamine in H_2SO_4 according to the method described by Sekiya *et al.* (1982) and Zhang *et al.* (2009), with some modifications. Leaves (0.5 g) were ground and extracted in 5 ml of phosphate buffer solution (pH 6.8, 50 mM) containing 0.1 M EDTA and 0.2 M ascorbic acid. The homogenate was mixed with 0.5 ml of 1 M HCl in a test tube to release H_2S, and H_2S was absorbed in a 1% (w/v) zinc acetate (0.5 ml) trap which is located in the bottom of the test tube. After 30 min of reaction, 0.3 ml of 5 mM dimethyl-*p*-phenylenediamine dissolved in 3.5 mM H_2SO_4 was added to the trap. Then 0.3 ml of 50 mM ferric ammonium sulphate in 100 mM H_2SO_4 was injected into the trap. The amount of H_2S in zinc acetate traps was determined spectrophometrically at 667 nm after leaving the mixture for 15 min at room temperature. Blanks were prepared by the same procedures without the zinc acetate solution.

Enzyme activity assays

RuBISCO (EC 4.1.1.39) was extracted according to Sayre *et al.* (1979) with slight modification. *Spinacia oleracea* leaves (10 g) were ground at 4 °C with a pestle in a mortar containing a small amount of quartz sand and 10 ml of grinding buffer solution consisting of 40 mM TRIS-HCl (pH 7.6), 10 mM $MgCl_2$, 0.25 mM EDTA, and 5 mM glutathione. After centrifugation at 20 000 *g* for 15 min at 4 °C, the supernatant was used for the enzyme assay. RuBISCO activity was assayed using the methods of Huang and Bie (2010). The activities of OAS-TL (EC 2.5.1.47) and LCD (EC 4.4.1.-) were determined as described by Bloem *et al.* (2004).

SDS–PAGE and western blot analysis

Leaf samples (0.5 g) were ground in liquid N_2 with a mortar and pestle. Total protein were extracted with a buffer containing 50 mM phosphate buffer solution (pH 7.5), 2% β-mercaptoethanol, 100 mM EDTA, 1% PVPP (w/v), and 1% Triton X-100 (v/v). After 15 min centrifugation (4 °C, 15 000 *g*), the upper phase was transferred to a new centrifuge tube. Two volumes of TRIS-saturated phenol (pH 8.0) were added and then the mixture was further vortexed for 30 min. Proteins were precipitated by adding 5 vols of ammonium sulphate-saturated methanol, and incubated at –20 °C for at least 4 h. After centrifugation as described above, the protein pellets were re-suspended and rinsed with ice-cold methanol followed by washing with ice-cold acetone twice, and spun down at 15 000 *g* for 10 min at 4 °C after each washing. Finally the washed pellets were air-dried and recovered in the lysis buffer containing 62.5 mM TRIS-HCl (pH 6.8), 2% SDS (v/v), 10% glycerol (v/v), and 2% β-mercaptoethanol (v/v). Protein concentrations were quantified using the Bradford assay (Bradford, 1976).

For western blot analysis, proteins (30 μg from each sample) were separated by SDS–PAGE using 12% (w/v) acrylamide gels according to Laemmli (1970) and electrophoretically transferred to a polyvinylidene difluoride (PVDF) membrane for 50 min. The membrane was blocked overnight with western blocking buffer (TIANGEN, China). The protein blot was probed with a primary antibody of the RuBISCO large subunit (AS03 037-200, Agrisera, Sweden) at a dilution of 1:5000 for 4 h at room temperature with agitation. Then the blot was washed three times in phosphate-buffered saline with Tween-20 (PBST) solution containing 50 mM TRIS-HCl (pH 8.0), 150 mM NaCl, 0.05% Tween-20 (v/v), and followed by incubation with the secondary antibody (anti-rabbit IgG horseradish peroxidase conjugated, Abcam, UK, 1:5000 dilution) for 2 h at room temperature. β-Actin (1:5000; Santa Cruz, CA, USA) was used as an internal control. The blots were finally washed as above and developed with SuperSigmal West Pico Chemiluminescent Substrate (Pierce, USA) according to the manufacturer's instructions. Images of the blots were obtained using a CCD imager (FluorSMax, Bio-Rad, USA). The Quantity One software (Bio-Rad, Hercules, CA, USA) was used to determine the optical density. The comparative optical density was used to determine the relative amount of protein expression, with the expression of β-actin used as an internal control.

Total RNA extraction and gene expression analysis

Quantitative real-time RT-PCR (qRT-PCR) was used to investigate the effect of H_2S on the expression patterns of genes encoding RuBISCO large subunit (*RBCL*), small subunit (*RBCS*), ferredoxin thioredoxin reductase (*FTR*), ferredoxin (*FRX*), thioredoxin m (*TRX-m*), thioredoxin f (*TRX-f*), NADP-malate dehydrogenase (*NADP-MDH*), *O*-acetylserine(thiol)lyase (*OAS*), serine acetyltransferase (*SERAT*), glycolate oxidase (*GYX*), and cytochrome oxidase (*CCO*) in *S. oleracea* seedlings. Leaves (0.5 g) were frozen and ground in liquid nitrogen with 2% polyvinylpyrrolidone and extracted with 0.5 ml of RNA purification reagent (Invitrogen Inc., CA, USA) by following the manufacturer's procedure. The RNA concentration was determined by using an ultraviolet spectrophotometer (Cary 50, Varian, USA) and RNA integrity was detected by 1% agarose gel electrophoresis. Total RNAs were reverse-transcribed into first-strand cDNAs with an M-MLV reverse

transcriptase (TaKaRa, Dalian, China). A 10 µl real-time PCR contained the following: 0.6 µl of forward and reverse primers (Supplementary Table S1 available at *JXB* online; the concentrations were determined experimentally as suggested by the manufacturer), 1 µl of cDNA (equivalent to 10 ng of mRNA), and 5 µl of Faststart Universal SYBR Green Master (ROX, Mannheim, Germany). Amplification and detection of *RBCL*, *RBCS*, *FTR*, *FRX*, *TRX-m*, *TRX-f*, *NADP-MDH*, *OAS*, *SERAT*, *GYX*, and *CCO* double-stranded DNA (dsDNA) synthesis were performed using the PCR conditions as described in Supplementary Table S2. Three independent replicates were performed for each sample. The comparative threshold cycle (Ct) method was used to determine the relative amount of gene expression. The glyceraldehyde-3-phosphate dehydrogenase gene (*GADPH*) was used as an internal control. The mRNA transcriptional abundance value of *RBCL*, *RBCS*, *GYX*, and *CCO* was expressed as $2^{-\Delta\Delta Ct}$ (Livak and Schmittgen, 2001). The Rotor-gene-6000 Real-Time PCR system (Corbett Research, Mortlake, Australia) was used to run qRT-PCR.

Statistical analysis

For gas exchange and chlorophyll fluorescence measurements, at least six leaves were used. For physiological and biochemical analyses, at least three replicates were included. Statistical significance was tested by the one-way or two-way analysis of variance (ANOVA) procedure of SPSS 13.0 (SPSS Inc, Chicago, IL, USA), and results are expressed as the mean ±SE. Post-hoc comparisons were tested using the Tukey or *t*-test at a significance level of $P < 0.05$.

Results

H_2S rather than other sulphur-containing derivatives causes the chlorophyll content increase in S. oleracea

As the first step in investigating the role of H_2S in regulating plant photosynthesis, its effect on chlorophyll content in *S. oleracea* leaves was examined. In order to distinguish the role of H_2S from that of other sulphur-containing derivatives and sodium, a series of sulphur- and sodium-containing chemicals including NaHS, Na_2S, Na_2SO_4, Na_2SO_3, $NaHSO_4$, $NaHSO_3$, and NaAC were used to treat *S. oleracea* seedlings. After treatment for 30 d, Na^+ or other sulphur-containing compounds, which were used as controls of NaHS, did not cause as great an increase in chlorophyll content as NaHS (Fig. 1A). It was also observed that the leaf chlorophyll content of seedlings treated with 100 µM NaHS was much higher than that of other treatments. Furthermore, the H_2S generated from various chemicals was detected by a selective H_2S sensor (Fig. 1B). Consistently, it was found the H_2S generated from 100 µM NaHS was the highest among the chemicals. These results suggest that H_2S rather than other sulphur-containing compounds or sodium was responsible for the increase in chlorophyll content in *S. oleracea* after NaHS treatment. Therefore, NaHS was used as a donor of H_2S in the subsequent experiments.

Effects of NaHS on seedling growth and chlorophyll content of S. oleracea

Chlorophyll was measured as a parameter of photosynthesis. Figure 2A showed that NaHS at lower concentrations enhanced seedling growth, with 100 µM being the optimal concentration. Figure 2B also showed that the biomass reached a maximum under 100 µM NaHS treatment, which

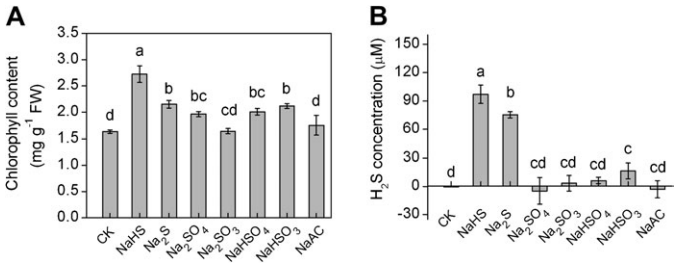

Fig. 1. (A) H_2S but not other sulphur- or sodium-containing compounds derived from NaHS contributed to increased chlorophyll content in *Spinacia oleracea* treated with half-strength Hoagland's nutrient solution containing 100 µM of different sulphur-containing compounds for 30 d. (B) H_2S generation from 100 µM of various sulphur- or sodium-containing compounds. The control (CK) was half-strength Hoagland's solution. Data are presented as the mean ±SE of four replicates. Columns labelled with different letters indicate significant differences at $P < 0.05$.

was ~2.6-fold higher than that of the control and a 146% increase as compared with the 10 µM NaHS treatment. In contrast, the biomass decreased by 55% and 37% at 500 µM and 1000 µM NaHS, respectively, compared with the control. Leaf soluble protein content exhibited a pronounced increase in various NaHS-treated seedlings compared with the untreated control (Fig. 2C). Figure 1 clearly shows that H_2S rather than other sulphur-containing derivatives enhances chlorophyll content. Here, the dose effect of NaHS on chlorophyll content was also explored. Figure 2D revealed that the chlorophyll content and chl *a*/*b* reached their maximum under 100 µM NaHS treatment, with an ~2.2- and 1.2-fold increase as compared with the control. Based on the above results, 100 µM is the optimal concentration for NaHS-induced seedling growth and chlorophyll accumulation; higher concentration of NaHS could be toxic for plant growth as reflected by the results in Fig. 2A and B.

Effect of NaHS on chloroplast ultrastructure

To evaluate further the role of NaHS in photosynthesis, transmission electron microscopy was used to analyse the changes in ultrastructure of chloroplasts after the application of NaHS. It was found that the number of grana lamellae stacking into functional chloroplasts significantly increased in leaves of 100 µM NaHS-treated seedlings compared with the control or 10 µM NaHS-treated seedlings (Fig. 3A, C). In contrast, under 1000 µM NaHS treatment, the number of grana lamellae stacking into functional chloroplasts was obviously decreased compared with 100 µM NaHS-treated leaves (Fig. 3D). These results suggest that 100 µM NaHS has a promoting effect and higher concentrations have inhibiting effects on the number of grana lamellae stacking into functional chloroplasts in *S. oleracea*.

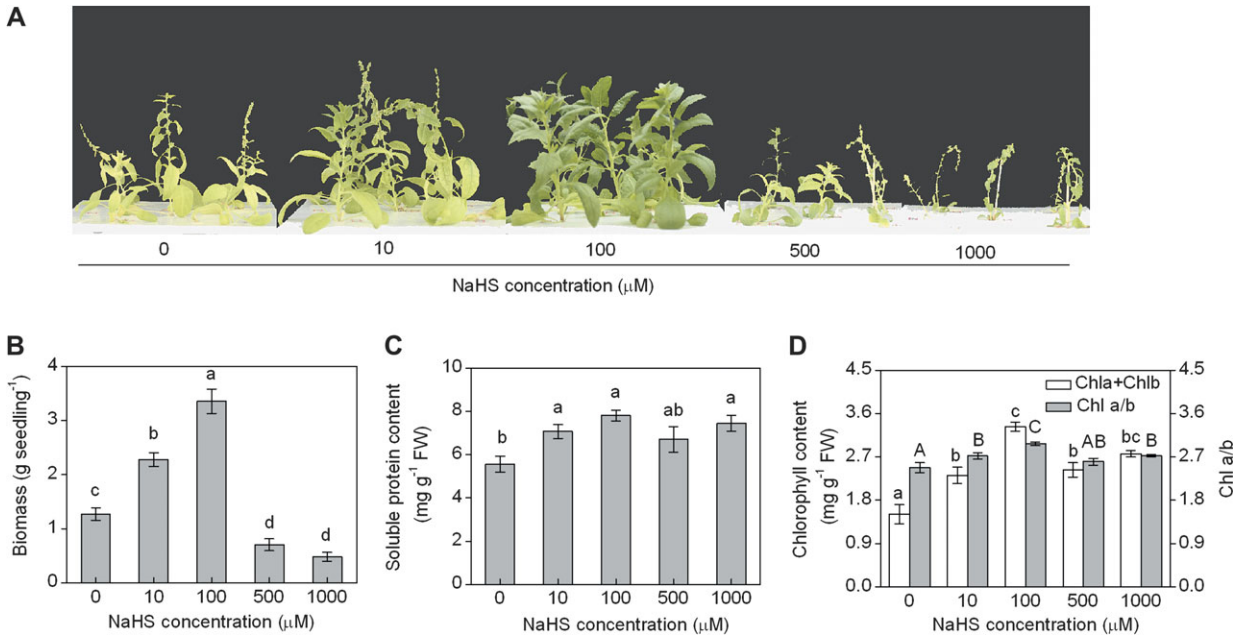

Fig. 2. Effects of H_2S on the phenotype (A), biomass (B), soluble protein (C), and chlorophyll content and chl *a/b* (D) in *Spinacia oleracea*. Data in B–D are presented as the mean ±SE of four replicates. Columns labelled with different letters indicate significant differences at P <0.05.

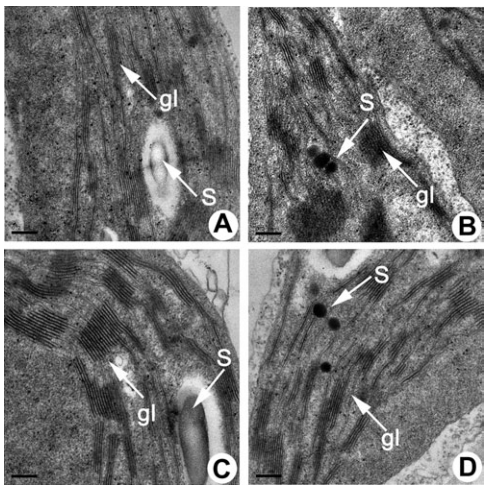

Fig. 3. Transmission electron microscopy analysis of the effect of NaHS on the chloroplast ultrastructure of *Spinacia oleracea*. (A) Control; (B) 10 μM NaHS; (C) 100 μM NaHS; (D) 1000 μM NaHS; gl, grana lamellae. S, starch. Bar=0.2 μm.

Effects of NaHS on the photosynthetic rate and chlorophyll fluorescence of S. oleracea leaves

In order to investigate the effect of NaHS on seedling photosynthetic characteristics further, Pn and g_s of leaves were measured at 800 μmol m^{-2} s^{-1} PAR with treatments using different NaHS concentrations. Pn and g_s reached a maximum under 100 μM NaHS treatment (Fig. 4A). Further, light–response curves and CO_2–response curves indicated that Pn was obviously higher in NaHS-treated seedlings than in the control (Fig. 4C, D). Chlorophyll fluorescence measurements showed that F_v/F_m and F_v/F_o were much higher in the NaHS-treated seedlings than in the the control (Fig. 4B). In addition, the *R*d, *L*cp, *L*sp, *AQE*, and *P*max of seedlings were calculated by modelling the response of leaf *P*n to PAR by a non-rectangular hyperbola and the *CE* was acquired by a rectangular hyperbola (Table 1). No effect of donor NaHS on *AQE* was found. However, *R*d and *L*cp were lower under NaHS treatment than in the control, whereas *P*max, *L*sp, and *CE* were notably higher under NaHS treatment. All these results suggest that seedling photosynthetic characteristics were significantly affected by 100 μM NaHS treatment.

Effects of NaHS on RuBISCO activity and RuBISCO LSU protein expression

In order to clarify the mechanism of H_2S-enhanced photosynthesis biochemically, the effects of different NaHS concentrations on the expression of RuBISCO LSU were analysed by protein western analysis. As shown in Fig. 5A and B, after quantification and normalization to β-actin, the protein expression level of RuBISCO LSU reached the maximal values under 10 μM and 100 μM NaHS treatments, which were 1.6- and 1.58-fold higher than the control, respectively. These data suggest that H_2S enhanced photosynthesis probably through up-regulating the protein expression of RuBISCO LSU. In addition, there was a significant increase in RuBISCO activity in response to 10 μM and 100 μM NaHS treatment (Fig. 5C). In brief, the H_2S-enhanced photosynthesis may be attributed to the increased protein expression of RuBISCO LSU and improved RuBISCO activity in a certain range of NaHS concentrations.

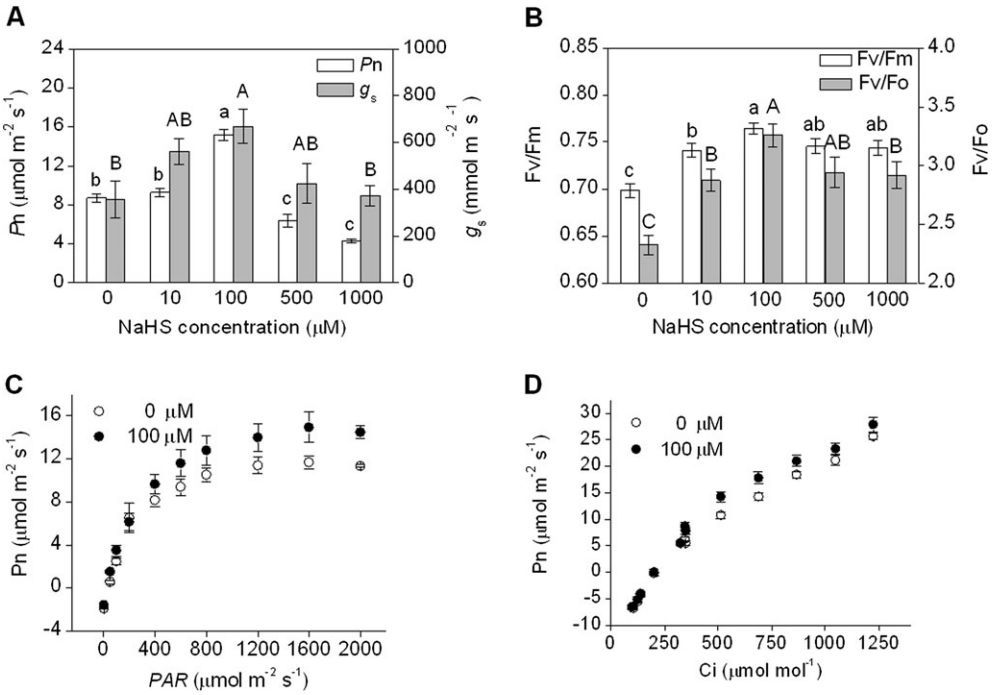

Fig. 4. Effects of H_2S on net photosynthetic rate (*Pn*) and stomatal conductance (g_s) (A), chlorophyll fluorescence (B), light–response curves (C), and intercellular CO_2–response curves (D) of *Spinacia oleracea*. Data are presented as the mean ±SE of six replicates. Columns labelled with different letters indicate significant differences at P <0.05.

Table 1. Effects of the H_2S donor NaHS on the apparent quantum yield (*AQE*), dark respiration (*Rd*), low light compensation point (*Lcp*), high light saturation point (*Lsp*), maximum net photosynthetic rate (Pmax), and carboxylation efficiency (*CE*) of *Spinacia oleracea* seedlings

Data are presented as the mean ±SE. The significant level of difference between control and treatment is indicated by * for P <0.05 and ** for P <0.01.

Variables	Control	100 μM NaHS
AQE	0.060±0.007	0.060±0.008
Rd (μmol CO_2 m^{-2} s^{-1})	2.09±0.12	1.46±0.17*
Lcp (μmol m^{-2} s^{-1})	35.6±2.7	24.7±2.4*
Lsp (μmol m^{-2} s^{-1})	296.0±10.3	389.7±15.8**
Pmax (μmol CO_2 m^{-2} s^{-1})	14.53±0.24	18.36±0.84*
CE (mol m^{-2} s^{-1})	0.087±0.001	0.108±0.001*

Effects of NaHS on RBCL and RBCS gene expression

To evaluate further the molecular response of *S. oleracea* photosynthesis to H_2S, the genes encoding the RuBISCO large and small subunits were analysed at the transcriptional level using qRT-PCR. The expression of *RBCL* and *RBCS* was normalized by using *GADPH* as a reference gene. Figure 6A showed that the relative gene expression abundance of *RBCL* in leaves of *S. oleracea* treated with 10 μM and 100 μM NaHS was higher than in the control (0 μM NaHS). Figure 6B and C showed the time course change of *RBCL* and *RBCS* expression in leaves of *S. oleracea* treated with 100 μM NaHS for 0, 6, 12, 24, and 36 h. The *RBCL* expression reached the maximal value at 24 h of NaHS treatment, being 1.91-fold higher than that of the control (0 h) (Fig. 6B). Similarly, the *RBCS* expression was also increased by 158% at 36 h of NaHS treatment compared with the control (0 h) (Fig. 6C).

Effects of NaHS on thiol content and gene expression related to thiol redox modification

To study further whether exogenously applied NaHS has an effect on thiol redox modification of proteins involved in photosynthesis, the total NPTs, GSH, and cysteine content was measured. As shown in Table 2, NaHS treatment resulted in an obvious increase in thiol content. Moreover, the expression of genes related to thiol redox modification in chloroplasts including *FTR*, *FRX*, *TRX-m*, *TRX-f*, and *NADP-MDH* was also obviously increased under NaHS treatment (Fig. 7A–E).

Effects of NaHS on endogenous H_2S production

A high accumulation of endogenous H_2S in *S. oleracea* seedling leaves caused by exogenously applied NaHS was observed (Table 2). To evaluate further the role of NaHS in sulphide metabolism in plant, the activity of several key enzymes in sulphide metabolism was measured. As shown in Table 2, the activities of OAS-TL and LCD were increased by NaHS treatment. Further, the expression of *OAS* and *SERAT* genes encoding OAS-TL and serine acetyltransferas (SAT), respectively, was measured in *S. oleracea* treated with NaHS. As shown in Fig. 7F and G, the expression abundance of *OAS* was obviously increased under NaHS treatment, whereas that of *SERAT* was reduced.

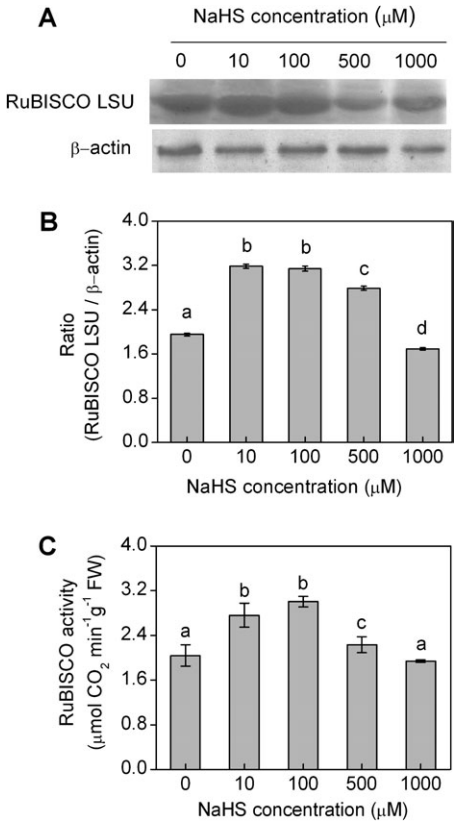

Fig. 5. Western blot analysis of ribulose-1,5-bisphoshate carboxylase large subunit (RuBISCO LSU) of *Spinacia oleracea* treated with 0, 10, 100, 500, and 1000 μM NaHS for 30 d (A). The relative expression level is shown as the RuBISCO LSU/β-actin ratio with the analysis by Quantity One software (B). RuBISCO activities of *Spinacia oleracea* treated with 0, 10, 100, 500, and 1000 μM NaHS for 30 d (C). Data are presented as the mean ±SE of three replicates. Columns labelled with different letters indicate significant differences at P <0.05.

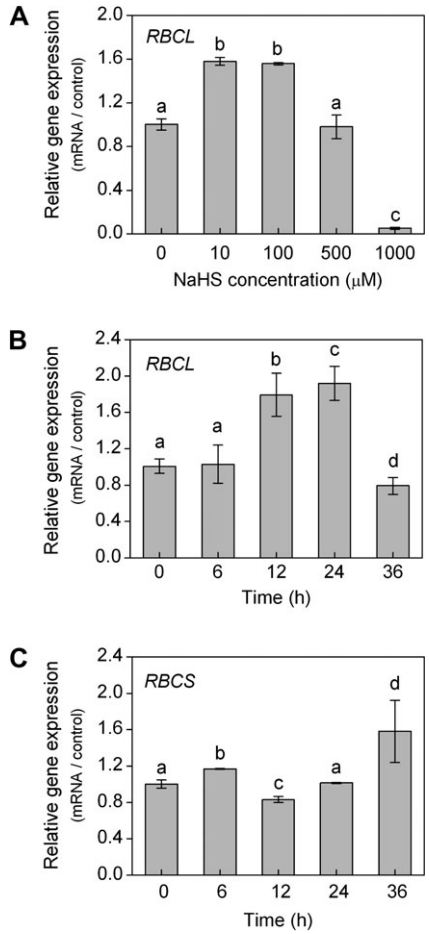

Fig. 6. Gene expression of *RBCL* of *Spinacia oleracea* seedlings treated with various concentrations of NaHS (0, 10, 100, 500, and 1000 μM) in half-strength Hoagland's nutrient solution for 30 d (A), and the effects of H_2S on *RBCL* and *RBCS* gene expression in seedlings treated with 100 μM NaHS in half-strength Hoagland's nutrient solution for 0, 6, 12, 24, and 36 h (B and C). The relative mRNA level of each gene was normalized to the mRNA of *GADPH*. Data are presented as the mean ±SE of three replicates. Columns labelled with different letters indicate significant differences at P <0.05.

Effects of NaHS on GYX and CCO gene expression

Based on the above photosynthesis data related to *R*d and *L*cp, the gene expression of *GYX* and *CCO* in *S. oleracea* seedlings treated with the optimal NaHS concentration was further analysed. As shown in Fig. 7H and I, the relative expression abundance of *GYX* and *CCO* was significantly decreased under NaHS treatment compared with the control, suggesting that the light and dark respiration could be reduced by the given concentration of NaHS.

Discussion

H_2S affected chlorophyll content, plant growth, and chloroplast ultrastructure

NaHS has been widely used as an H_2S donor in animal research (Hosoki *et al.*, 1997). It dissolves in water and dissociates to produce Na^+ and HS^-, then HS^- associates with H^+ to form H_2S. In this report, other sulphur-containing components such as S^{2-}, SO_4^{2-}, SO_3^{2-}, HSO_4^-,

Table 2. Effects of the H_2S donor NaHS on non-protein thiols (NPTs), glutathione (GSH), cysteine, endogenous H_2S content, O-acetylserine(thiol)lyase (OAS-TL), and L-cysteine desulphydrase (LCD) activities of *Spinacia oleracea* seedlings

Data are presented as the mean ±SE. The significant level of the difference between control and treatment is indicated by * for P < 0.05 and ** for P <0.01.

Variables	Control	100 μM NaHS
NPTs (μmol g^{-1} FW)	2.69±0.04	4.47±0.23**
GSH (nmol g^{-1} FW)	221.6±5.8	360.5±31.9*
Cysteine (nmol g^{-1} FW)	6.46±0.53	8.55±0.18*
Endogenous H_2S content (μmol g^{-1} FW)	0.041±0.007	0.107±0.015**
OAS-TL (nmol Cys mg^{-1} protein min^{-1})	609.9±26.7	724.4±20.7*
LCD (nmol H_2S mg^{-1} protein min^{-1})	22.38±0.74	28.36±0.96*

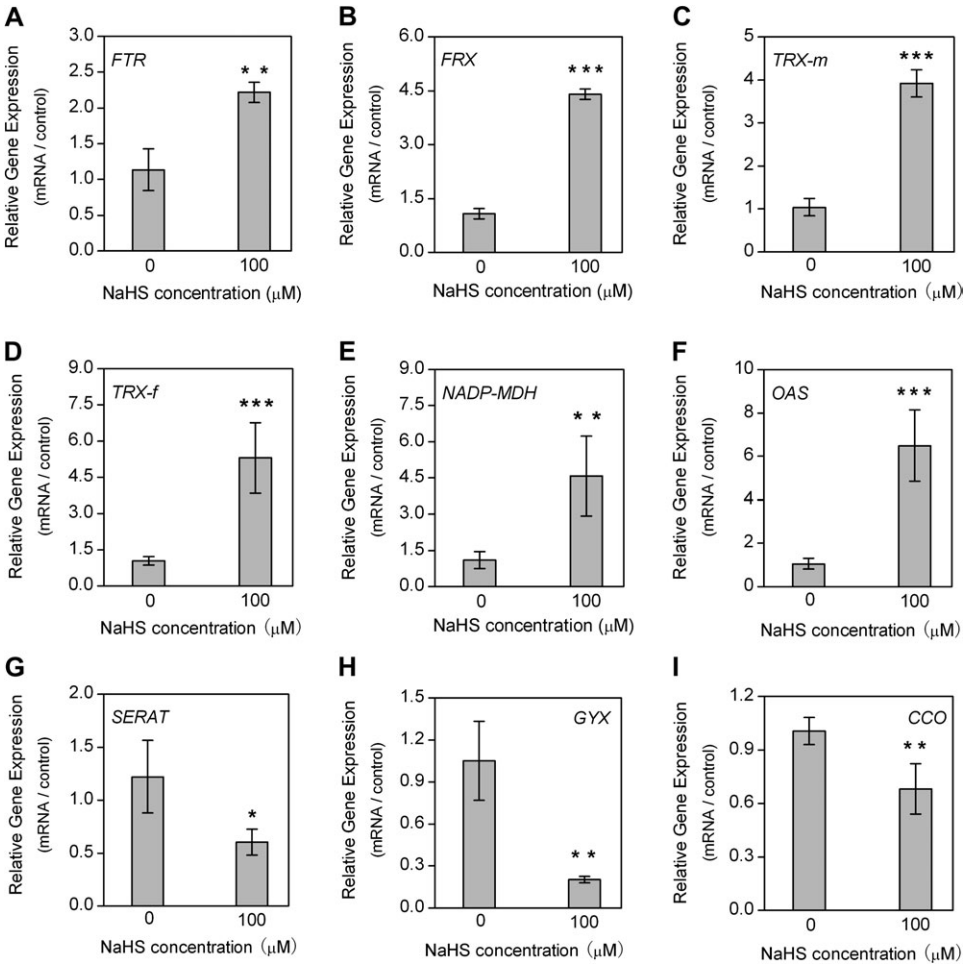

Fig. 7. Effects of H_2S on ferredoxin thioredoxin reductase (*FTR*) (A), ferredoxin (*FRX*) (B), thioredoxin m (*TRX-m*) (C), thioredoxin f (*TRX-f*) (D), NADP-malate dehydrogenase (*NADP-MDH*) (E), *O*-acetylserine(thiol)lyase (*OAS*) (F), serine acetyltransferase (*SERAT*) (G), glycolate oxidase (*GYX*) (H), and cytochrome oxidase (*CCO*) (I) gene expression in *Spinacia oleracea* seedlings treated with 100 μM NaHS in half-strength Hoagland's nutrient solution. The relative mRNA level of each gene was normalized to the mRNA of *GADPH*. Data are presented as the mean ±SE of three replicates. The significant level of difference between control and treatment is indicated by *, ** and *** for $P < 0.05$, $P < 0.01$ and $P < 0.001$, respectively.

HSO_3^-, and Na^+ were used as the controls of NaHS, but none of them was able to increase the chlorophyll content of *S. oleracea* (Fig. 1A). Meanwhile, in order to understand the actual H_2S generation from these chemicals used, the H_2S generation by various sulphur-containing chemicals was directly analysed using a selective H_2S sensor (Fig. 1B). It was found that the H_2S generated from NaHS was the highest among all the chemicals tested under the same measuring conditions including pH, temperature, time, volume, solution, and so on. Although Na_2S also generated H_2S, it was not steady within the measurement period used here (Supplementary Fig. S2 at *JXB* online). Furthermore, NaHS promoted the chlorophyll content, photosynthesis, and growth of *S. oleracea* in a dose-dependent manner (Figs 2A, 4; Table 1), which is consistent with the observations by other researchers that H_2S affected chlorophyll content and enhanced the embryo root length of *Pisum sativum* (Zhang *et al.*, 2009; Li *et al.*, 2010). It is well known that the chlorophyll content and photosynthetic rate are closely correlated in plants. The result implies that H_2S may play an important role in promoting photosynthesis in *S. oleracea*.

In animal cells, low concentrations of H_2S have been proven to function as a signalling molecule (Wang, 2002). Therefore, it is important to clarify whether H_2S also plays a role in modulating physiological processes in plants. Recently, it was demonstrated that H_2S may act as an antioxidant to counteract oxidative stresses induced by copper, boron, and aluminium toxicity (Zhang *et al.*, 2008, 2010; Wang *et al.*, 2010) as well as osmotic stress in plants (Zhang *et al.*, 2009). In addition, a recent report demonstrated that H_2S induces stomatal closure and participates in the abscisic acid (ABA)-dependent signalling pathway by regulating ATP-binding cassette (ABC) transporters in guard cells (García-Mata and Lamattina 2010). In the present study, it was revealed that 100 μM NaHS increased seedling biomass, and soluble protein and chlorophyll content in *S. oleracea*. However, a high NaHS concentration decreased these parameters (Fig. 2). In addition, the number of grana lamellae in functional chloroplasts was

also significantly increased by 100 μM NaHS treatment compared with the control and other NaHS concentrations (Fig. 3A, C). These results suggest that 100 μM NaHS could promote the biogenesis of chloroplasts by increasing the number of grana lamellae and the biosynthesis of chlorophyll, which will lead to an enhancement of photosynthesis.

H_2S affected photosynthetic characteristics in S. oleracea

The function of a low concentration of H_2S in plant photosynthesis is still not clear. Data from the present experiments showed that H_2S may be involved in the regulation of photosynthesis as 100 μM NaHS enhances while a higher concentration inhibits the photosynthesis of *S. oleracea* (Fig. 4A). These results are in accordance with the data from previous studies showing that excess H_2S negatively affects plant growth by inhibiting mitochondrial electron transport and photosynthesis in plants (Beauchamp *et al.*, 1984; Lin and Sternberg, 1992).

Further analysis on photosynthetic features revealed that *P*n reached maximum values under 100 μM NaHS treatment compared with the control and treatments with other NaHS concentrations (Fig. 4A, D). *P*max was also significantly higher in NaHS-treated seedlings than in the control (Table 1). This result is important for clarifying the effect of H_2S on photosynthesis because a higher *P*max allows seedlings to acquire a higher potential to assimilate carbon dioxide. *AQE* reflects the light use efficiency of plants at low light intensities. No significant difference in *AQE* between the control and 100 μM NaHS-treated plants was observed, suggesting that NaHS treatment could not enhance the light use efficiency of *S. oleracea* at a lower light intensity. *L*sp represents the capacity of plants to use the maximal light. The results showed that 100 μM NaHS can enhance the maximal light use of *S. oleracea* under a high light intensity. On the other hand, as *L*cp is the light value at which the rate of CO_2 fixation by photosynthesis is equal to the rate of CO_2 release by respiration and photorespiration, a lower *L*cp reflects a lower respiration and a higher RuBISCO carboxylase activity or lower RuBISCO oxygenase activity (Nunes *et al.*, 2009). Some studies have reported that a sharp increase in *L*cp can be induced by drought, water deficit, and infective disease (Shen *et al.*, 2007; Nunes *et al.*, 2009). The obvious decrease in *L*cp in 100 μM NaHS-treated seedlings observed in the present study (Table 1) implies that NaHS could enhance photosynthesis and the accumulation of organic compounds in *S. oleracea* seedlings. In addition, the sharp decrease in *R*d under 100 μM NaHS (Table 1) indicates that NaHS-treated *S. oleracea* seedling had lower respiration compared with the control. As cytochrome oxidase is the terminal oxidase in respiration and glycolate oxidase is the first enzyme in photorespiration, the changes in the mRNA expression of these enzymes were analysed by qRT-PCR (Fig. 7H, I). The results showed that the mRNA expression of these two enzymes was inhibited significantly by 100 μM NaHS treatment. These findings allow the conclusion to be reached that the decrease in *R*d by H_2S may be due to the decrease of the cytochrome oxidase level. This hypothesis is in agreement with a previous study which suggested that the mitochondria cytochrome oxidase activity was obviously inhibited by H_2S as well as NO and CO in mammalian cells (Cooper and Brown, 2008).

In plant responses to changed environment or external signals, leaf photosynthesis is often altered due to changes in g_s and/or *CE* in mesophyll cells (Yuan and Xu, 2001). In the present study, the increases in *P*n and *CE* of *S. oleracea* leaves caused by 100 μM NaHS (Fig. 4A; Table 1) can be explained by both the increased g_s and the H_2S-induced enhancement in the carboxylation process, as the enhancement of *CE* has been considered to play a major role in the improvement of photosynthesis (Pell *et al.*, 1992; Farage and Long, 1999).

Changes of photochemical efficiency

Chlorophyll fluorescence is a measure of PSII function and light harvesting efficiency. The F_v/F_m in dark-adapted leaves is recognized as a good indicator of a photo-inhibitory or photo-oxidative effect on PSII (Maxwell and Johnson, 2000). The F_v/F_m and F_v/F_o increased significantly in *S. oleracea* treated with 100 μM NaHS (Fig. 4B), indicating that the photochemical reaction in PSII was partially increased, which is consistent with the increase in chlorophyll content caused by 100 μM NaHS treatment (Fig. 2D). Chlorophyll contributes greatly to the light harvesting and primary photochemical reaction in plants (Yan *et al.*, 2010) and chlorophyll content correlates closely to the F_v/F_m and F_v/F_o. In agreement with a previous study showing that excess sulphide (1 mM) inhibited the activity of PSII in cyanobacteria and tobacco chloroplasts (Oren *et al.*, 1979), the present results also indicated that a high concentration of sulphide has harmful effects on PSII in plants.

Changes in enzyme activity and gene expression of RuBISCO

RuBISCO is a key enzyme controlling photosynthetic carbon fixation in plants, and the level of activated RuBISCO is closely related to the *L*sp, *CE*, and the rate of photosynthetic carbon assimilation (Seemann and Berry, 1982; Lin and Hsu, 2004). The present results showed that the protein expression of RuBISCO LSU reached the highest level under 10 μM and 100 μM NaHS (Fig. 5A, B). Meanwhile, a significant increase in RuBISCO activity was observed at 100 μM NaHS treatment (Fig. 5C), suggesting that the improvement in photosynthesis under 100 μM NaHS treatment was a result of an increase in RuBISCO level.

To evaluate further the molecular effect of the H_2S donor NaHS on photosynthesis of *S. oleracea*, the changes at the transcriptional level of *RBCL* and *RBCS* were investigated using qRT-PCR. The results showed that the expression of *RBCL* and *RBCS* was significantly up-regulated by 100 μM

NaHS even within a short time (Fig. 6A–C), suggesting that RuBISCO biosynthesis is very sensitive to H_2S treatment. Taken together, all the evidence presented here indicates that the positive effect of 100 μM NaHS on leaf photosynthesis occurs mainly through stimulating the transcription of *RBCL* and *RBCS* mRNA and enhancing the accumulation and activity of RuBISCO.

NaHS treatment causes changes in the level of total thiols and gene expression related to thiol redox modification

Previous studies have shown that in plants treated with H_2S, H_2S is rapidly incorporated into organic sulphur compounds, resulting in an increase in soluble thiols including GSH and cysteine (Schutz *et al.*, 1991). In the present study, it was found that the NPTs, GSH, and cysteine contents were significantly increased in *S. oleracea* after treatment with the optimal concentration of NaHS. Miginiac-Maslow *et al.* (2000) addressed the importance of thiol redox modification in photosynthetic electron transfer. It is well known that the ferredoxin/thioredoxin system in chloroplasts is critical for regulation of CO_2 assimilation in oxygenic photosynthesis (Buchanan, 1991). The ferredoxin/thioredoxin system, consisting of ferredoxin, ferredoxin-thioredoxin reductase (FTR), and thioredoxin (m and f), is a general mechanism of light-mediated enzyme regulation (Buchanan, 1991). Ferredoxin is reduced in the light by photosynthetic electron transfer at the level of PSI. It reduces FTR, generating a dithiol that reduces the disulphide bridge of thioredoxin. The very reactive dithiol of reduced thioredoxin m (named for its effectiveness in NADP-MDH activation) and f [named for its effectiveness in fructose-1,6-bisphosphatase (FBPase) activation] reduces the disulphides of NADP-MDH and FBPase, respectively, which shifts from a totally inactive to a fully active form (Ramaswamy *et al.*, 1999). In the present study, the gene expression of proteins in the ferredoxin/thioredoxin system, including ferredoxin, FTR, and thioredoxin (m and f), was obviously increased due to the higher content of thiols (Fig. 7A–D and Table 2), and the expression of *NADP-MDH*, which is strictly regulated by light through the ferredoxin/thioredoxin system, was also significantly increased under NaHS treatment (Fig. 7E). Since the ferredoxin/thioredoxin system in chloroplasts is quite important for regulation of CO_2 assimilation in oxygenic photosynthesis (Buchanan, 1991), the data led to the conclusion that H_2S not only functions as a signalling molecule, but is also involved in thiol redox modification to impact on the photosynthetic CO_2 assimilation in *S. oleracea*.

Endogenous H_2S production in NaHS-treated S. oleracea

In this study, the externally applied NaHS led to an increase in the internal concentration of H_2S in *S. oleracea* leaves (Table 2), which is similar to the results observed by other researchers (Zhang *et al.*, 2008, 2010). Further enzymatic analyses indicated that the externally applied NaHS significantly enhanced the activity of OAS-TL but only slightly enhanced that of the LCD enzyme (Table 2). Consistent with this, qRT-PCR experiments revealed that the expression of the *OAS* gene was significantly enhanced by the NaHS treatment (Fig. 7F), but not that of the *SERAT* gene (Fig. 7G). Since OAS-TL and LCD are responsible for H_2S release, and OAS-TL, LCD, and SAT control the cysteine levels in plants (Riemenschneider *et al.*, 2005), the NaHS-induced increase in the cysteine and H_2S levels in the present study could be largely due to the enhancement of the OAS-TL enzyme activity and gene expression instead of that of LCD and SAT. Therefore, the results suggest that externally supplied NaHS is also involved in sulphide metabolism.

In summary, the present results indicated that the increase in net leaf photosynthesis caused by 100 μM NaHS is mainly due to the enhanced expression and activity of RuBISCO and proteins involved in thiol redox modification. In addition, Pmax, CE, g_s, Lsp, and F_v/F_m were all obviously increased by 100 μM NaHS treatment, which will further enhance photosynthesis. Finally, 100 μM NaHS treatment resulted in a significant increase in plant biomass, chlorophyll content, soluble protein content, and the number of grana lamellae in chloroplasts. Taken together, these findings highlight an important role for H_2S in regulating leaf photosynthesis by possibly increasing the quantity and activity of RuBISCO, enhancing photosynthetic electron transfer through thiol redox modification, improving chloroplast biogenesis, etc. Further studies are needed to clarify the other photosynthetic processes affected by H_2S and to dissect the signaling pathways by which H_2S mediates the photosynthesis enhancement.

Supplementary data

Supplementary data are available at *JXB* online.

Figure S1. Electrochemical detection of H_2S concentration performed under various NaHS concentrations using an H_2S-selective electrode.

Figure S2. Electrochemical detection of H_2S concentration performed under 100 μM NaHS and Na_2S for 30 min using an H_2S-selective electrode.

Table S1. Sequences of the forward and reverse primers used in qRT-PCR for gene expression analysis in *Spinacia oleracea* seedlings treated with the H_2S donor NaHS.

Table S2. Procedures of dsDNA synthesis used in qRT-PCR for gene expression analysis in *Spinacia oleracea* seedlings treated with the H_2S donor NaHS.

Acknowledgements

We are grateful to Ting-Wu Liu, Bing-Bo Li, and Wei-Zhi Lu for assistance with experiments, and Mrs Sieh Sorie Kargbo and Thadee Vuguziga for critically reading the

manuscript. This study was financially supported by the Natural Science Foundation of China (NSFC 30930076), the Foundation of the Chinese Ministry of Education (20070384033), the Program for New Century Excellent Talents in Xiamen University, Changjiang Scholarship, a Research Grant Council of the Hong Kong Special Administrative Region (project codes 465009 and 465410), and direct grants from the Chinese University of Hong Kong.

References

Batasheva S, Abdrakhimov F, Bakirova G, Isaeva E, Chikov V. 2010. Effects of sodium nitroprusside, the nitric oxide donor, on photosynthesis and ultrastructure of common flax leaf blades. *Russian Journal of Plant Physiology* **57,** 376–381.

Beauchamp RO, Bus JS, Popp JA, Boreiko CJ, Andjelkovich DA, Leber P. 1984. A critical review of the literature on hydrogen sulfide toxicity. *Critical Reviews in Toxicology* **13,** 25–97.

Benavides GA, Squadrito GL, Mills RW, Patel HD, Isbell TS, Patel RP, Darley-Usmar VM, Doeller JE, Kraus DW. 2007. Hydrogen sulfide mediates the vasoactivity of garlic. *Proceedings of the National Academy of Sciences, USA* **104,** 17977–17982.

Bloem E, Riemenschneider A, Volker J, Papenbrock J, Schmidt A, Salac I, Haneklaus S, Schnug E. 2004. Sulphur supply and infection with *Pyrenopeziza brassicae* influence l-cysteine desulphydrase activity in *Brassica napus* L. *Journal of Experimental Botany* **55,** 2305–2312.

Buchanan BB. 1991. Regulation of CO_2 assimilation in oxygenic photosynthesis: the ferredoxin/thioredoxin system: perspective on its discovery, present status, and future development. *Archives of Biochemistry and Biophysics* **288,** 1–9.

Bradford MM. 1976. A rapid and sensitive method for the quantitation of microgram quantities of protein utilizing the principle of protein–dye binding. *Analytical Biochemistry* **72,** 248–254.

Chang CS, Li YH, Chen LT, *et al*. 2008. LZF1, a HY5-regulated transcriptional factor, functions in *Arabidopsis* de-etiolation. *The Plant Journal* **54,** 205–219.

Cooper C, Brown G. 2008. The inhibition of mitochondrial cytochrome oxidase by the gases carbon monoxide, nitric oxide, hydrogen cyanide and hydrogen sulfide: chemical mechanism and physiological significance. *Journal of Bioenergetics and Biomembranes* **40,** 533–539.

Dean C, Pichersky E, Dunsmuir P. 1989. Structure, evolution, and regulation of RbcS genes in higher plants. *Annual Review of Plant Physiology and Plant Molecular Biology* **40,** 415–439.

Del Longo OT, Gonzalez CA, Pastori GM, Trippi VS. 1993. Antioxidant defences under hyperoxygenic and hyperosmotic conditions in leaves of two lines of maize with differential sensitivity to drought. *Plant and Cell Physiology* **34,** 1023–1028.

Farage PK, Long SP. 1999. The effects of O_3 fumigation during leaf development on photosynthesis of wheat and pea: an *in vivo* analysis. *Photosynthesis Research* **59,** 1–7.

García-Mata C, Lamattina L. 2010. Hydrogen sulphide, a novel gasotransmitter involved in guard cell signalling. *New Phytologist* **188,** 977–984.

Hosoki R, Matsuki N, Kimura H. 1997. The possible role of hydrogen sulfide as an endogenous smooth muscle relaxant in synergy with nitric oxide. *Biochemical and Biophysical Research Communications* **237,** 527–531.

Huang X, Bie Z. 2010. Cinnamic acid-inhibited ribulose-1, 5-bisphosphate carboxylase activity is mediated through decreased spermine and changes in the ratio of polyamines in cowpea. *Journal of Plant Physiology* **167,** 47–53.

Jin CW, Du ST, Zhang YS, Tang C, Lin XY. 2009. Atmospheric nitric oxide stimulates plant growth and improves the quality of spinach (*Spinacia oleracea*). *Annals of Applied Biology* **155,** 113–120.

Kong WW, Zhang LP, Guo K, Liu ZP, Yang ZM. 2010. Carbon monoxide improves adaptation of *Arabidopsis* to iron deficiency. *Plant Biotechnology Journal* **8,** 88–99.

Kosower NS, Kosower EM, William B, Jakoby OWG. 1987. Thiol labeling with bromobimanes. *Methods in Enzymology* **143,** 76–84.

Krantev A, Yordanova R, Janda T, Szalai G, Popova L. 2008. Treatment with salicylic acid decreases the effect of cadmium on photosynthesis in maize plants. *Journal of Plant Physiology* **165,** 920–931.

Krause GH, Weis E. 1991. Chlorophyll fluorescence and photosynthesis: the basics. *Annual Review of Plant Physiology and Plant Molecular Biology* **42,** 313–349.

Laemmli UK. 1970. Cleavage of structural proteins during the assembly of the head of bacteriophage T4. *Nature* **227,** 680–685.

Li D, Xiao Z, Liu L, Wang J, Song G, Bi Y. 2010. Effects of exogenous hydrogen sulfide (H_2S) on the root tip and root border cells of *Pisum sativum*. *Chinese Bulletin of Botany* **45,** 354–362 (in Chinese with English abstract).

Li L, Bhatia M, Moore PK. 2006. Hydrogen sulphide—a novel mediator of inflammation? *Current Opinion in Pharmacology* **6,** 125–129.

Lichtenthaler HK. 1987. Chlorophylls and carotenoids: pigments of photosynthetic biomembranes. *Methods in Enzymology* **148,** 350–382.

Lin G, Sternberg L. 1992. Effect of growth form, salinity, nutrient and sulfide on photosynthesis, carbon isotope discrimination and growth of red mangrove (*Rhizophora mangle* L.). *Functional Plant Biology* **19,** 509–517.

Lin MJ, Hsu BD. 2004. Photosynthetic plasticity of *Phalaenopsis* in response to different light environments. *Journal of Plant Physiology* **161,** 1259–1268.

Livak KJ, Schmittgen TD. 2001. Analysis of relative gene expression data using real-time quantitative PCR and the $2^{-\Delta\Delta Ct}$. *Methods* **25,** 402–408.

Lloyd D. 2006. Hydrogen sulfide: clandestine microbial messenger? *Trends in Microbiology* **14,** 456–462.

Maxwell K, Johnson GN. 2000. Chlorophyll fluorescence—a practical guide. *Journal of Experimental Botany* **51,** 659–668.

Miginiac-Maslow M, Johansson K, Ruelland E, *et al*. 2000. Light-activation of NADP-malate dehydrogenase: a highly controlled process for an optimized function. *Physiologia Plantarum* **110,** 322–329.

Nishimura K, Ogawa T, Ashida H, Yokota A. 2008. Molecular mechanisms of RuBisCO biosynthesis in higher plants. *Plant Biotechnology* **25,** 285–290.

Nunes C, Araújo SS, Silva JM, Fevereiro P, Silva AB. 2009. Photosynthesis light curves: a method for screening water deficit resistance in the model legume *Medicago truncatula*. *Annals of Applied Biology* **155,** 321–332.

Olsson T, Leverenz JW. 1994. Non-uniform stomatal closure and the apparent convexity of the photosynthetic photon flux density response curve. *Plant, Cell and Environment* **17,** 701–710.

Oren A, Padan E, Malkin S. 1979. Sulfide inhibition of photosystem II in cyanobacteria (blue-green algae) and tobacco chloroplasts. *Biochimica et Biophysica Acta* **546,** 270–279.

Pell EJ, Eckardt N, Enyedp JA. 1992. Timing of ozone stress and resulting status of ribulose bisphosphate carboxylase/oxygenase and associated net photosynthesis. *New Phytologist* **120,** 397–405.

Prioul JL, Chartier P. 1977. Partitioning of transfer and carboxylation components of intracellular resistance to photosynthetic CO_2 fixation: a critical analysis of the methods used. *Annals of Botany* **41,** 789–800.

Ramaswamy S, Saarinen M, Lemaire-Chamley M, Issakidis-Bourguet E, Miginiac-Maslow M, Eklund H. 1999. Structural basis for light activation of a chloroplast enzyme: the structure of sorghum NADP-malate dehydrogenase in its oxidized form. *Biochemistry* **38,** 4319–4326.

Rennenberg H. 1983. Role of *O*-acetylserine in hydrogen sulfide emission from pumpkin leaves in response to sulfate. *Plant Physiology* **73,** 560–565.

Riemenschneider A, Nikiforova V, Hoefgen R, De Kok LJ, Papenbrock J. 2005. Impact of elevated H_2S on metabolite levels, activity of enzymes and expression of genes involved in cysteine metabolism. *Plant Physiology and Biochemistry* **43,** 473–483.

Sayre RT, Kennedy RA, Pringnitz DJ. 1979. Photosynthetic enzyme activities and localization in *Mollugo verticillata* populations differing in the levels of C_3 and C_4 cycle operation. *Plant Physiology* **64,** 293–299.

Schutz B, De Kok LJ, Rennenberg H. 1991. Thiol accumulation and cysteine desulfhydrase activity in H_2S-fumigated leaves and leaf homogenates of cucurbit plants. *Plant and Cell Physiology* **32,** 733–736.

Seemann JR, Berry JA. 1982. Interspecific differences in the kinetic properties of RuBP carboxylase protein. *Carnegie Institute Washington Year Book* **81,** 78–83.

Sekiya J, Schmidt A, Wilson LG, Filner P. 1982. Emission of hydrogen sulfide by leaf tissue in response to l-cysteine. *Plant Physiology* **70,** 430–436.

Shen H, Hong L, Ye W, Cao H, Wang Z. 2007. The influence of the holoparasitic plant *Cuscuta campestris* on the growth and photosynthesis of its host *Mikania micrantha*. *Journal of Experimental Botany* **58,** 2929–2937.

Suzuki Y, Kihara-Doi T, Kawazu T, Miyake C, Makino A. 2010. Differences in Rubisco content and its synthesis in leaves at different positions in *Eucalyptus globulus* seedlings. *Plant, Cell and Environment* **33,** 1314–1323.

Wang BL, Shi L, Li YX, Zhang WH. 2010. Boron toxicity is alleviated by hydrogen sulfide in cucumber (*Cucumis sativus* L.) seedlings. *Planta* **231,** 1301–1309.

Wang R. 2002. Two's company, three's a crowd: can H_2S be the third endogenous gaseous transmitter? *FASEB Journal* **16,** 1792–1798.

Westerman S, De Kok LJ, Stuiver CEE, Stulen I. 2000. Interaction between metabolism of atmospheric H_2S in the shoot and sulfate uptake by the roots of curly kale (*Brassica oleracea*). *Physiologia Plantarum* **109,** 443–449.

Wilson LG, Bressan RA, Filner P. 1978. Light-dependent emission of hydrogen sulfide from plants. *Plant Physiology* **61,** 184–189.

Wirtz M, Droux M, Hell R. 2004. *O*-Acetylserine (thiol) lyase: an enigmatic enzyme of plant cysteine biosynthesis revisited in *Arabidopsis thaliana*. *Journal of Experimental Botany* **55,** 1785–1798.

Yamaguchi K, Nishimura M. 2000. Reduction to below threshold levels of glycolate oxidase activities in transgenic tobacco enhances photoinhibition during irradiation. *Plant and Cell Physiology* **41,** 1397–1406.

Yan K, Chen W, Zhang GY, Xu S, Liu ZL, He XY, Wang LL. 2010. Elevated CO_2 ameliorated oxidative stress induced by elevated O_3 in *Quercus mongolica*. *Acta Physiologiae Plantarum* **32,** 375–385.

Yang G, Wu L, Jiang B, *et al*. 2008. H_2S as a physiologic vasorelaxant: hypertension in mice with deletion of cystathionine γ-lyase. *Science* **322,** 587–590.

Yuan L, Xu DQ. 2001. Stimulation effect of gibberellic acid short-term treatment on leaf photosynthesis related to the increase in Rubisco content in broad bean and soybean. *Photosynthesis Research* **68,** 39–47.

Zelitch I, Ochoa S. 1953. Oxidation and reduction of glycolic and glyoxylic acids in plants. I. Glycolic and oxidase. *Journal of Biological Chemistry* **201,** 707–718.

Zelitch I, Schultes NP, Peterson RB, Brown P, Brutnell TP. 2009. High glycolate oxidase activity is required for survival of maize in normal air. *Plant Physiology* **149,** 195–204.

Zhang H, Hu LY, Hu KD, He YD, Wang SH, Luo JP. 2008. Hydrogen sulfide promotes wheat seed germination and alleviates oxidative damage against copper stress. *Journal of Integrative Plant Biology* **50,** 1518–1529.

Zhang H, Ye YK, Wang SH, Luo JP, Tang J, Ma DF. 2009. Hydrogen sulfide counteracts chlorophyll loss in sweetpotato seedling leaves and alleviates oxidative damage against osmotic stress. *Plant Growth Regulation* **58,** 243–250.

Zhang H, Tan ZQ, Hu LY, Wang SH, Luo JP, Jones RL. 2010*a*. Hydrogen sulfide alleviates aluminum toxicity in germinating wheat seedlings. *Journal of Integrative Plant Biology* **52,** 556–567.

Zhao W, Zhang J, Lu Y, Wang R. 2001. The vasorelaxant effect of H_2S as a novel endogenous gaseous K_{ATP} channel opener. *The EMBO Journal* **20,** 6008–6016.